Chemical Looping Combustion and Chemical Looping with Oxygen Uncoupling Experiments in a Batch Reactor Using Spray-Dried CaMn1–xMxO3 (M = Ti, Fe, Mg) Particles as Oxygen Carriers

Chemical-Looping Combustion and Chemical-Looping with Oxygen Uncoupling experiments in a batch reactor using spray dried $CaMn_{(1-x)}M_xO_{3-\delta}$ (M=Ti, Fe, Mg) particles as Oxygen Carrier

Peter Hallberg(♣), Dazheng Jing(♠), Magnus Rydén(♣), Tobias Mattisson(♣), Anders Lyngfelt(♣)*

(♣)Department of Energy and Environment, (♠)Department of Chemical and Biological Engineering

Chalmers University of Technology, S-41296 Göteborg, Sweden

Chemical-Looping Combustion and Chemical-Looping with Oxygen Uncoupling (CLOU) with oxygen carrier particles consisting of $CaMn_{(1-x)}M_xO_{3-\delta}$ (M=Ti, Fe, Mg) has been studied by consecutive oxidation and reduction experiments in a fluidized-bed batch reactor. The examined particles were produced by spray drying and all did show significant release of gas phase oxygen to inert atmosphere at 900 and 1000°C. All particles also provided very high reactivity with syngas and methane. Some of the examined particles showed unfavourable fluidization characteristics, i.e. formed dust during operation or showed agglomeration or defluidization tendencies. The crushing strength of the particles that formed dust was typically below 1.2 N.

The desired perovskite structure was detected in all samples by X-ray diffractometry. The materials that included iron and titanium had these elements incorporated in the perovskite structure, substituting manganese. When magnesium had been included it was not incorporated into the crystal structure but rather present as a separate phase of MgO. In addition to a perovskite phase most samples also contained small amounts of marokite, $CaMn_2O_4$. Particles doped with MgO calcined at 1300°C showed good fluidization behaviour, as well as particularly high reactivity with fuel.

Introduction:

Anthropogenic climate change caused by emission of so called greenhouse gases has received significant attention in the past decades. Among greenhouse gases emitted by human activities Carbon dioxide (CO_2) is considered to have the largest effect on climate change. The concentration of CO_2 in atmosphere has risen to about 390 ppm in 2010 compared with 280 ppm in the pre-industrial era, mainly due to emissions of CO_2 from combustion of fossil fuel. Apart from climate change, increasing amount of atmospheric CO_2 could lead to other negative effects on the earth as well, such as ocean acidification and loss of biodiversity. Therefore, decreasing CO_2 emission from combustion of fossil fuels has become an urgent task.

Renewable energy sources such as solar, wind and hydro power may provide opportunities to do so in the future, but the current huge demand for fossil fuels suggests that such fuels still will be the predominant energy source in coming decades.

One possible way to reduce emissions of CO_2 from fossil fuel combustion is so called Carbon Capture and Storage. Basically, CO_2 could be captured at point sources such as power plants and

transported to certain storage sites, where it could be stored and prevented from reaching the atmosphere. This way, it would be possible to continue to generate heat and power by combustion of fossil fuels, without contributing to climate change. Examples of potential storage sites are deep saline aquifers and depleted natural gas fields. Most technologies for capturing CO_2 include large scale gas separation and thus involve considerable costs and also a distinct energy penalty. Chemical looping combustion (CLC) with inherent separation of CO_2 could possibly provide cheaper and more efficient CO_2 capture compared to the alternatives[1].

Chemical Looping Combustion

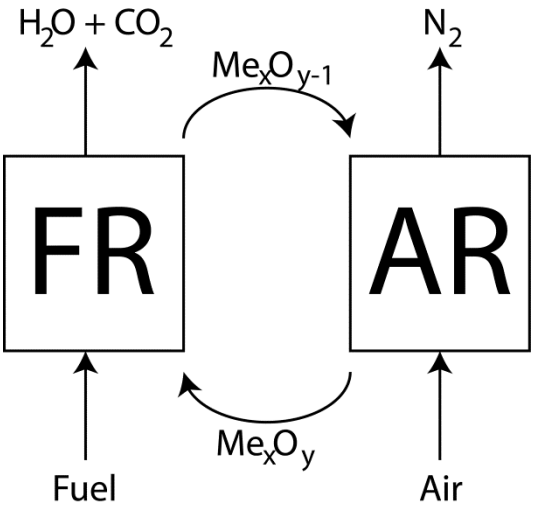

Figure 1 Schematic description of the Chemical Looping Combustion process. FR and AR denote fuel and air reactor. Me_xO_y and Me_xO_{y-1} are the oxidized and reduced oxygen carrier.

Chemical-Looping Combustion is a method to oxidize fuels with inherent capture of CO_2. In CLC, the oxygen needed to oxidize the fuel is provided with a solid oxygen carrier material. This is different from conventional combustion in which oxygen is provided by mixing air and fuel. A CLC system is comprised of two reactors, one fuel reactor and one air reactor. In the fuel reactor,

oxygen carrier particles react with hydrocarbon fuels producing CO_2 and H_2O as flue gases, reaction (1). This way, almost pure CO_2 is obtained after steam has been removed by condensation. The process is described in *figure 1*.

$$C_nH_{2m} + (2n + m)\ Me_xO_y \rightarrow nCO_2 + mH_2O + (2n + m)\ Me_xO_{y-1} \quad (1)$$

The reduced oxygen carrier is transferred to the air reactor where it is oxidized by air (reaction 2).

$$O_2 + 2Me_xO_{y-1} \rightarrow 2Me_xO_y \quad (2)$$

After reoxidation, the oxygen carrier is ready to be transferred back to fuel reactor for further reaction cycles.

CLC is meant to be conducted in a cyclic fashion, with continuous flow of oxygen carrier between the air and fuel reactor. The sum of reaction (1) and reaction (2) is combustion of the fuel with oxygen, so the amount of heat generated is exactly the same as in an ordinary combustion process. Moreover, since fuel and air is not mixed directly, CO_2 is produced undiluted with N_2 from the air. As CO_2 and H_2O are easily separated by cooling and condensation of steam to liquid water, this means that there is no direct energy penalty compared to ordinary combustion for obtaining pure CO_2. This is a huge advantage compared to other techniques for CO_2 capture, for which energy consuming processes are required to separate N_2 from flue gases or air.

While there are many possible ways to realize chemical-looping combustion, the most commonly proposed setup is to use circulating fluidized-bed reactors[1, 2]. Such reactor systems allow a smooth flow of solid material between the reactor vessels and also provide very good contact between gases and solids. Circulating fluidized-bed reactors are currently used for a range of large-scale applications such as combustion of solid fuels and fluid catalytic cracking.

Chemical Looping with Oxygen Uncoupling (CLOU)

In CLC, it is assumed that the main mechanism for oxidation of the fuel is gas-solid reactions between the fuel and the oxygen carrier. So if solid fuels such as coal or biomass are to be used, they need to be gasified in order to be oxidized by a solid oxygen carrier. Alternatively, it would be possible to use an oxygen carrier capable of releasing gas phase oxygen at fuel reactor conditions, shown in *reaction 3*.

$$2Me_xO_y \rightarrow O_2 + 2Me_xO_{y-1} \qquad (3)$$

Reaction 3 could provide gas phase oxygen for direct fuel oxidation. In fact, released O_2 would react with the fuel in a normal combustion reaction. The total reaction for this set of reactions would be the same as in chemical-looping combustion, but the reaction mechanism for fuel oxidation would be different. The concept is usually referred to as chemical looping with oxygen uncoupling (CLOU). It has been shown that the overall reaction rate for oxidation of solid fuels can be an least an order of magnitude faster than for ordinary CLC involving char gasification with CO_2 or steam[3, 4].

CLOU was first suggested in a patent by Lyngfelt and Mattisson[5] and later in a publication by Mattisson et al.[6]. Although particularly well suited for solid fuel applications, this process may be advantageous for oxidation of gaseous fuels as well, as having gas phase oxygen in the fuel reactor might facilitate complete conversion of such fuels.

Oxygen carrier materials:

In a Chemical Looping system, a crucial matter is the nature of the solid oxygen carrier[7, 8]. To select suitable oxygen carriers several parameters should be considered. One important parameter is reactivity towards fuels. High conversion of fuels such as natural gas or syngas is required. This includes both high theoretical conversion, which is dependent on the thermodynamic properties of the oxygen carrier, and fast reaction kinetics, which can be dependent on many factors (size, porosity, surface area etc.).

Another important factor is reversibility, which can be expressed for example as the number of fuel conversion cycles an oxygen carrier can undergo without deactivation. Other important parameters include resistance towards attrition and fragmentation, which for example can be described as the number of times a particle can pass through a cyclone at certain velocity without being grind to dust. Moreover, factors such as melting temperature, oxygen transfer capacity, price, toxicity and environmental impact should also be considered.

Transition metal oxides such as for instance iron oxide, nickel oxide, copper oxide and manganese oxide are all potential oxygen carriers, as is combined metal oxides of different transition metals. NiO-based oxygen carriers have been proven satisfactory in numerous studies, e. g.[9 - 13]. The use of NiO involves several drawbacks though, such as thermodynamic constraints concerning the degree of fuel conversion, sensitivity to fuel impurities such as sulphur and compared to alternatives high price and toxicity[14]. Due to these drawbacks, the development of oxygen carrier materials without nickel is a good development.

One combined metal oxide that has been proposed as oxygen carrier for CLC is $CaMnO_{3-\delta}$, and various alterations of it[15 - 17]. $CaMnO_{3-\delta}$ is of perovskite structure, i.e. a crystalline structure which has a unit cell which can be written $ABO_{3-\delta}$ in which A is a large cation and B is a smaller

cation. The δ-factor expresses the degree of oxygen deficiency in the structure, and is zero for a perfect structure.

Perovskites differ from other oxygen carriers that undergo distinct phase change, i. e. CuO – Cu_2O, Ni – NiO, Fe_2O_3 – Fe_3O_4. In materials of perovskite structure, there is no distinct phase change. Instead, materials of perovskite structure are feasible for chemical-looping applications because δ can be increased or reduced by altering factors in the surroundings such as temperature, pressure or O_2 fugacity, see Leonidova et al.[18] The surroundings in a chemical-looping air reactor are oxidative, while they are reductive in the fuel reactor. Therefore δ_{ar} will be smaller and δ_{fr} will be larger. The amount of O_2 available for oxidation of fuel can be written as $(\delta_{fr} - \delta_{ar})$, see reaction (4).

$$ABO_{3-\delta ar} \leftrightarrow ABO_{3-\delta fr} + \tfrac{1}{2}(\delta_{fr}-\delta_{ar})\, O_2 \qquad (4)$$

The A and B sites does not have to consist of one single type of ions. Doping of the A and B site with one or more type of ions is possible as long as the dopants have similar ionic radii and oxidation state as the main atom. The B site can be selected among most transition metals. Good candidates for the application chemical-looping combustion could be for example manganese, iron and titanium. The A site needs to have much larger ionic radii and there are less options. Calcium appears to be the most attractive for the A site due to good availability and low cost. The general criteria's concerning formability of perovskites has been extensively reviewed by Li et al.[19]

Another notable feature of $CaMnO_{3-\delta}$ is that the sum of reactions in the chemical-looping fuel reactor will be slightly exothermic which could be advantageous with respect to heat balance of a

chemical-looping facility. Reaction enthalpy for O_2 release from $CaMnO_{3-\delta}$ materials have been examined by Rørmark et al.[20]

In the materials tested in this paper some of the manganese was substituted by titanium, iron or magnesium. Of these, titanium and iron ions are close to a manganese ion in size and shape and could be expected to become incorporated in the perovskite structure at the B site. This is not the case for magnesium, for which the ions are too large to fit at the B site but too small to fit at the A site. Therefore magnesium can be expected to be present in a separate MgO phase in the particles. The effect of B site doping on the properties of an oxygen carrier material is not obvious. In general, addition of different dopants or could be expected to affect the O_2-conductivity of the perovskite and possibly also induce certain catalytic qualities.

An overview of the topic perovskite based oxygen carrier materials for chemical looping applications can be found in a recent paper by Rydén et al.[21]

Not all materials of perovskite structure undergo changes at conditions relevant for chemical looping, but $CaMnO_{3-\delta}$ based materials has been shown to do so[15, 16], as well as materials substituted with La and Fe[22, 23].Another notable feature of $CaMnO_{3-\delta}$ based materials is that reaction (1) is slightly exothermic which could be advantageous with respect to heat balance of a chemical-looping facility. Previous tests of $CaMnO_{3-\delta}$ showed that there was decomposition to $Ca_2MnO_{4-\delta}$ and $CaMn_2O_4$[24] hence alterations were maybe in an attempt to stabilize the structure. In the materials tested in this paper some of the manganese was substituted by titanium, iron or magnesium.

Experimental

Oxygen carrier materials

The oxygen carriers examined in this work were manufactured at VITO in Belgium by spray-drying. Commercially available manganese oxide, calcium hydroxide and a small amount of titanium oxide, iron oxide or magnesium oxide were used as raw materials, see *table 1*.

Table 1 *Designations, chemical compositions and recipes (wt%) for the oxygen carrier particles examined in this study*

Particle	**Mn_3O_4**	**$Ca(OH)_2$**	**TiO_2**	**Fe_2O_3**	**MgO**
C9 - $CaMn_{0.75}Ti_{0.25}O_{3-\delta}$	37.8	49	13.2	-	-
C10 - $CaMn_{0.95}Ti_{0.05}O_{3-\delta}$	48.1	48.1	2.6	-	-
C11 - $CaMn_{0.8}Fe_{0.2}O_{3-\delta}$	40.4	49	-	10.6	-
C12 - $CaMn_{0.9}Fe_{0.1}O_{3-\delta}$	45.5	49.2	-	5.3	-
C13 - $CaMn_{0.8}Mg_{0.2}O_{3-\delta}$	42.6	51.8	-	-	5.6
C14 - $CaMn_{0.9}Mg_{0.1}O_{3-\delta}$	46.8	50.5	-	-	2.7

Following the spray drying process, separate batches of each particle composition were calcined at 1100, 1200 and 1300 °C for 4 h. The resulting particles were then sieved into different size fractions. The diameter of the particles used for CLOU and reactivity testing as well as XRD and light microscope investigation was 125-180 µm. Crushing strength testing was measured on particles in the size range 180 – 212 µm using a Shimpo FGN-5 apparatus. A crushing strength below a certain threshold would suggest that the particles could easily break apart. Each sample was also inspected by eye, with the help of a light microscope, to detect possible micro agglomerations, satellites on particles or other anomalies. Each sample was also examined by X-ray diffractometry, in order to determine phases present. This was done for oxidized fresh particles and for used samples, as will be explained below.

Experimental procedure

The experiments in this study were performed on a reactor system with setup according to *figure 2*. The experimental setup was similar to what have been used in some earlier studies[9, 25].

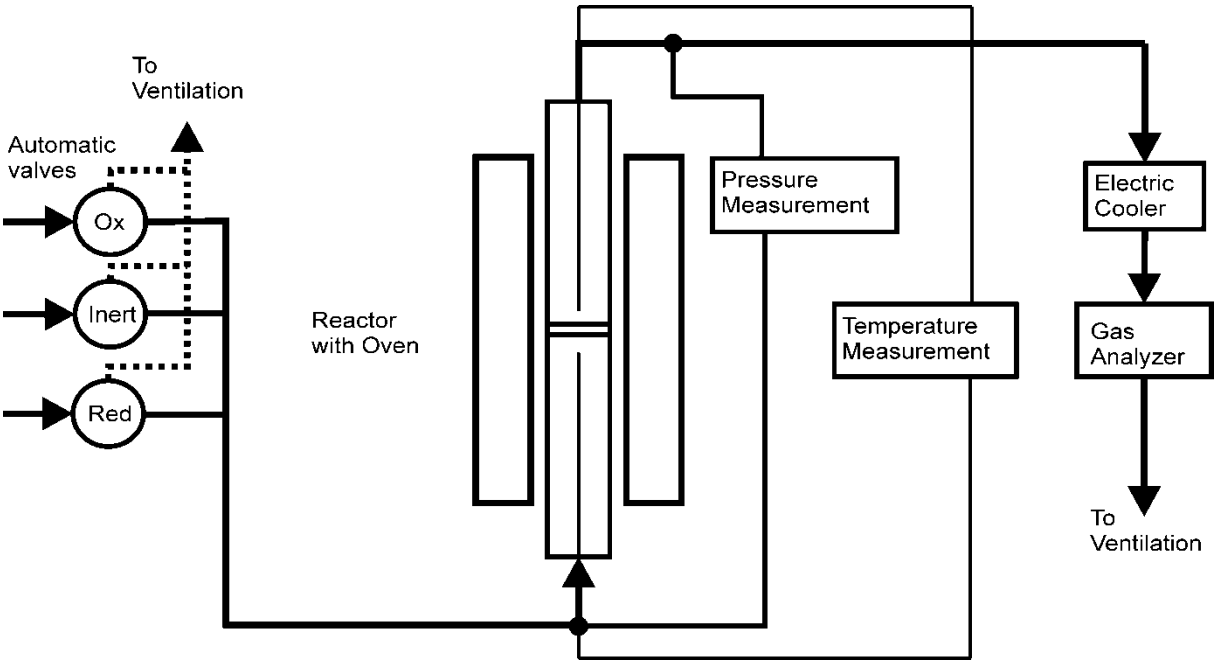

Figure 2 Schematic description of the experimental setup

The experimental procedure was as follows. A small fluidized bed reactor of quartz was placed inside an electric oven, in order to be able to maintain the temperature at the desired level over the course of the experiment. The oven was insulated and the openings through which the gases entered and exited the reactor were insulated with quartz wool. The quartz reactor was cylindrical and had an inner diameter of 22 mm and a height of 870 mm. The oxygen carrier particles were placed on a porous quartz plate located 370 mm from the lower end. 15 g oxygen carrier was used both for CLOU and reactivity testing. Temperature measurements were conducted with two CrAl/NiAl thermocouples enclosed in inconel-600 in quartz shells. The thermocouples were located 28 mm below the porous plate in order to measure temperature

below the bed, and 22 mm above for measurements in the bed. The experiments were performed at 900 – 1000 °C, as measured by the upper thermocouple.

Table 2 Experimental scheme for oxygen uncoupling and fuel reactivity tests. F_i is flow in the period i, i.e. Oxidation, Reduction and Inert. t_i is the time for period i. T is temperature.

No of cycles	Reducing gas	F_{Ox} [mL_N/min]	F_{In} [mL_N/min]	t_{In} [s]	F_{Red} [mL_N/min]	t_{Red} [s]	T_{Ox} [°C]	T_{Red} [°C]
3	nitrogen	900	600	360	-	-	900	900
1	nitrogen	900	600	360	-	-	900	900 → 1000
3	methane	900	600	60	450/360	20	950	950
3	syngas	900	600	60	450/360	80	950	950
3	nitrogen	900	600	360	-	-	900	900
2	nitrogen	900	600	360	-	-	900	900 → 1000
1	nitrogen	900	600	1800	-	-	900	900 → 1000

The CLOU properties of the different particles were studied by examining the oxygen release from oxidized particles in nitrogen, while fuel reactivity was investigated through reaction with methane and syngas. The experiments were run in cyclic fashion, in which a period of oxidation followed by a period of reduction constitute one cycle. Reduction was performed either with inert gas in order to examine O_2 release, or with fuel in order to examine fuel oxidation.

Most cycles were run multiple times in order to investigate if the reactivity would change as function of cycle due to irreversible reactions. The oxidation was conducted with a flow of 900 $mL_N\ min^{-1}$ (normalized to 1 bar and 25°C) of N_2 with 5 % O_2. The oxidation period was not operated for a fixed period. Instead, it was maintained until the sample was fully oxidized, i.e. until the ingoing oxygen concentration was the same as the outgoing. This was done in order to

make sure that degree of oxidation of the samples was the same prior to each reduction period. The fuel reduction was conducted with a flow of 450 mL_N min^{-1} of CH_4 or syngas ($CO:H_2$, 1:1) respectively. For the magnesium doped particles a methane flow of 360 mL_N min^{-1} was tested as well as 450 mL_N min^{-1} and the results were found to be similar with respect to fuel conversion (γ) as function of the degree of reduction (ω). In-between the oxidation and fuel reduction periods, a flow of N_2 was used to remove any remaining oxidizing or reducing gases. This inert period lasted 60 s and the flow rate during this period was 600 mL_N min^{-1}. The experimental scheme is presented in *table 2* and is similar to what has previously been used by Azimi et al.[25].

As can be seen in *figure 2*, the outlet stream from the reactor was cooled and water was condensed and removed prior to analysis. The dry gas was led to a Rosemount NGA2000 Multi-component gas analyser where the concentrations of CO, CO_2, CH_4 and O_2, as well as the volume flow of the dry gas, were measured. The gas concentrations, volume flow and temperature were recorded every two seconds. The pressure drop over the reactor was measured with a frequency of 20 Hz in order to determine whether the bed was fluidized or not.

Data evaluation

Reactivity with fuel of the different particles are expressed by γ, the carbon based conversion of the fuel, which is defined as follows:

$$\gamma = \frac{x_{CO_2}}{x_{CO_2}+x_{CO}+x_{CH_4}} \quad (5)$$

,where x_i is the volume fraction of compound x in the dry gas leaving exiting the reactor. Since the oxygen release, and thus conversion, of these particles is dependent on the degree of oxidation that is examined as well. The degree of oxidation is expressed as ω, which is defined as follows:

$$\omega = \frac{m}{m_{OX}} \qquad (6)$$

,where m is the actual mass of the oxygen carrier material and m_{OX} is the mass of the fully oxidized particle. In practice ω is calculated through a species balance over the reactor where it is assumed that no H_2 leaves the reactor. From the negligible amount of CO measured this assumption is reasonable. When methane is used as fuel the expression degree of oxidation, for time i, is calculated by:

$$\omega_i = \omega_{i-1} - \int_{t_{i-1}}^{t_i} \frac{\dot{n} M_O}{m_{OX}} \left(4x_{CO_2} + 3x_{CO}\right) dt \qquad (7)$$

and when syngas is used as fuel:

$$\omega_i = \omega_{i-1} - \int_{t_{i-1}}^{t_i} \frac{\dot{n} M_O}{m_{OX}} \left(2x_{CO_2} + x_{CO}\right) dt \qquad (8)$$

,where $\dot{n}$ is the molar flux of the dry gas leaving the reactor, M_O is the molar mass of oxygen.

Results and discussion

Crushing strength, effective density and some operational characteristics are shown in table 3. Effective density is measured as bulk density but space between the particles is excluded by assuming monodisperse spherical particles, i. e. a void fraction of 0.37.

Table 3. Crushing strength, density and some operational characteristics for examined oxygen-carrier particles.

Particle name	Calcination temperature (°C)	Effective density (kg m^{-3})	Crushing strength (N)	Defluidization (Yes/No)	Dust formation (Yes/No)
C9	1100	1123	0.46	-	-

	1200	1393	0.63	No	Yes
	1300	2274	1.3	Yes	No
C10	1100	1083	0.46	No	Yes
	1200	1506	0.68	No	Yes
	1300	2412	1.29	Yes	No
C11	1100	994	0.39	No	Yes
	1200	1649	1.11	No	Yes
	1300	2666	1.43	Yes	No
C12	1100	987	0.4	-	-
	1200	1419	0.97	No	Yes
	1300	2463	1.38	Yes	No
C13	1100	1001	0.36	No	Yes
	1200	1239	0.65	No	Yes
	1300	1705	1.28	No	No
C14	1100	1041	0.27	-	-
	1200	1438	0.56	No	yes
	1300	2255	1.38	No	No

The softest particles all formed dust in the reactor which was found in the coarse quartz wool filter in the top of the reactor. Dust formation in short experiments with low gas velocities indicate a very short particle life time in a real reactor system, where higher gas velocities would be necessary. Particle density was quite strongly correlated to crushing strength. From table 3 it can be seen that the threshold value for dust formation is crushing strength between 1.11 and 1.28 N or a density between 1649 and 1705 kg m^{-3}. C9-, C12- and C14-1100 of the materials calcined at 1100 °C were not tested in the batch reactor as they had very low crushing strength and could be expected to form dust, based on the results for the other materials. The materials

doped with Ti and Fe calcined at 1300 °C experienced some defluidization during operation. Defluidization was reversible and it was still possible to finish experiments which involved defluidization in good fashion. However, when particles which had involved defluidization were removed from the reactor agglomeration of various extents was discovered. The agglomeration ranged from small micro agglomerates consisting of a few particles to most of the bed being agglomerated. It can also be noted that the four particles which defluidized were the four particles with highest density. This is not unexpected since minimum fluidization velocity is a function of particle density. The Mg-doped C13-1300 and C14-1300 did not form dust or defluidize during operation.

Oxygen Uncoupling

The gas phase O_2-release (CLOU-effect) of the particles is shown in *figure 3a-c, expressed* as oxygen concentration as a function of the degree of oxidation of the sample. The figure shows the second of the three initial cycles, presented in *table 2*, with nitrogen as a reducing gas at 900 °C.

In figure 3a-c, it can be seen that the first phase of the oxygen uncoupling involved a sharp decline in oxygen concentration, compared to the oxidation phase which was operated with 5 % oxygen. To some extent this slope derives from the fact that there was not perfect plug flow in the reactor. That should however only account for part of the oxygen measured the first 5 - 10 seconds. Consequently, the rest of the oxygen originates from the oxygen carrier. In the start of the inert phase ω is large and oxygen is released comparably fast. As ω shrinks the rate of oxygen release decreases. While this behaviour fits with theory[21], it is different from experiments

with for example CuO based oxygen carriers which typically involve steady release of O_2 at a level equivalent to thermodynamic equilibrium[4].

The difference between the oxygen release in the six inert cycles at 900 °C were very small for all tested materials, which is illustrated in *Figure 4* for particle C10-1200. This indicates high experimental reproducibility and good reversibility of involved reactions.

In theory, the degree of oxidation should be a function of both O_2 partial pressure and temperature. At higher temperature, the degree of oxidation could be expected to be lower (corresponds to high δ-factor) and facilitate further O_2 release. In order to examine this phenomenon the temperature was increased to 1000 °C during one inert phase, as indicated in *table 2*, and indeed a larger oxygen release was observed. The difference is shown for particle C10-1200 in *figure 5*, and all examined materials showed similar behaviour. When the time of the inert cycle was increased the rate of oxygen release gradually approached zero. After 1800 s a ω-value of circa 0.99 was reached, which would correspond to a δ change of roughly 0.09. That ω heads towards this value suggest that the potential for oxygen uncoupling at this temperature is around 1 wt% of the particle mass. An example of this behaviour is given in *figure 6* for C13-1300, showing outgoing oxygen concentration and ω against time.

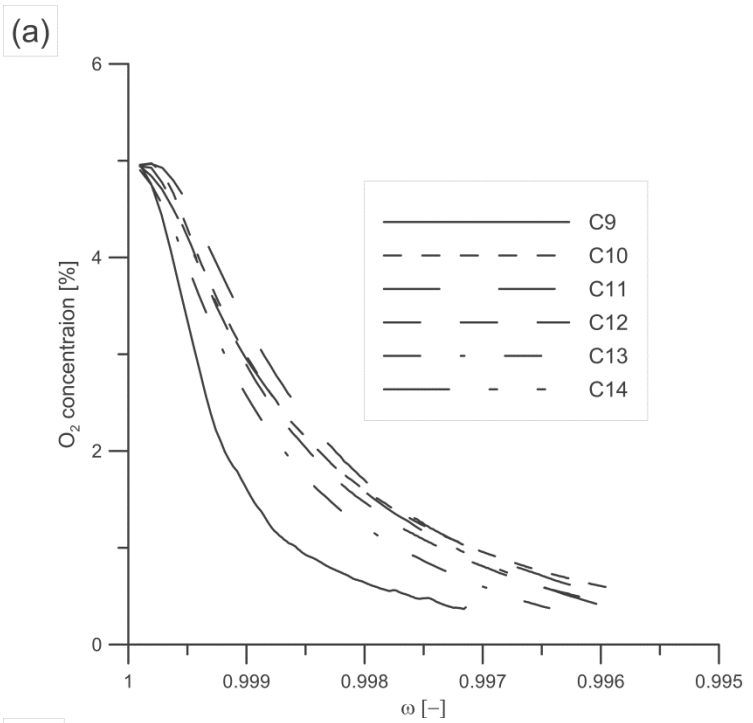
(a)
6
4
2
0
O_2 concentraion [%]
1
0.999
0.998
0.997
0.996
0.995
ω [–]
C9
C10
C11
C12
C13
C14

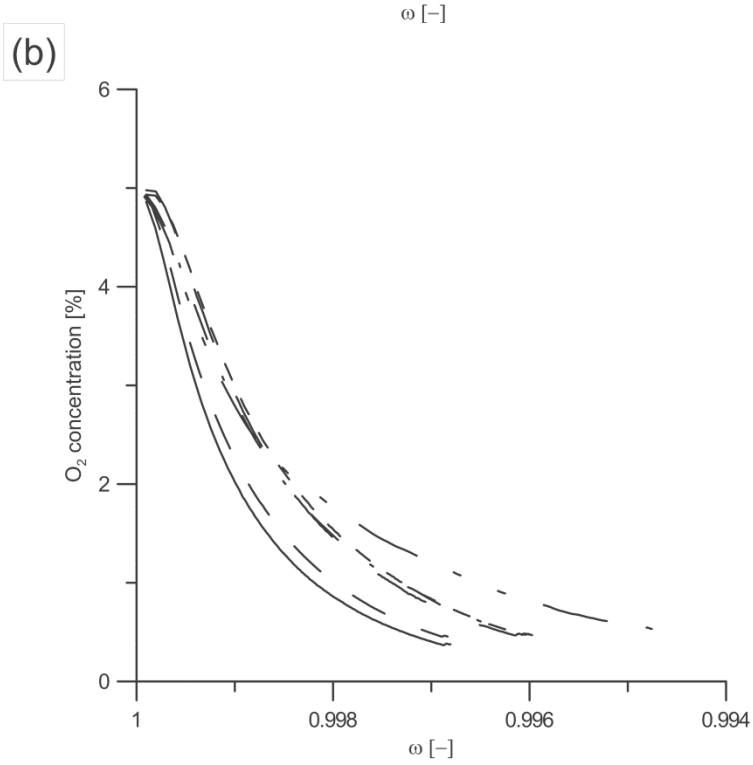
(b)
6
4
2
0
O_2 concentration [%]
1
0.998
0.996
0.994
ω [–]

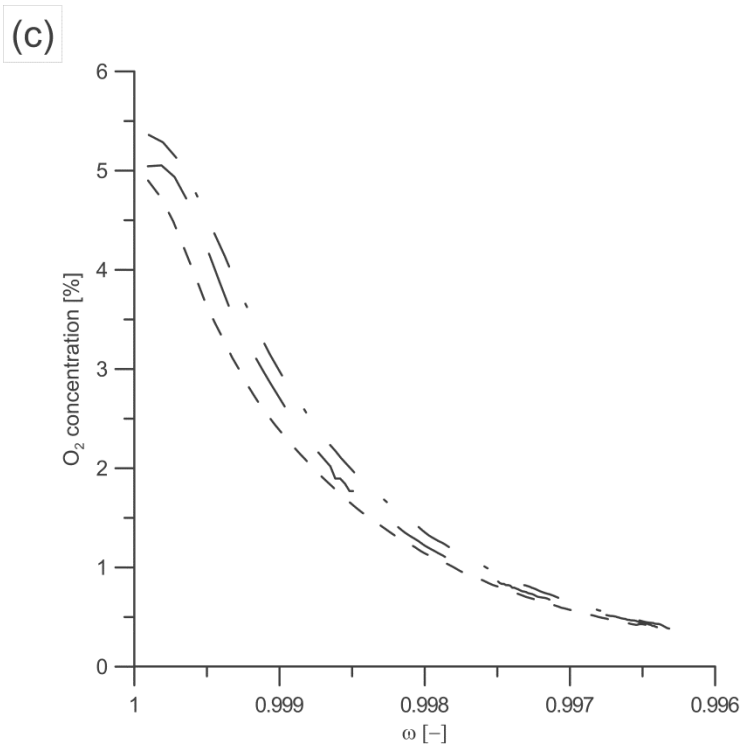

Figure 3 Oxygen released from particles as a function of degree of oxidation (ω) for particles calcined at 1300 (a), 1200 (b), 1100 °C (c). The graphs show the second the first three nitrogen cycles preformed at 900 °C presented in *table 2.* The reduction time is 360 s.

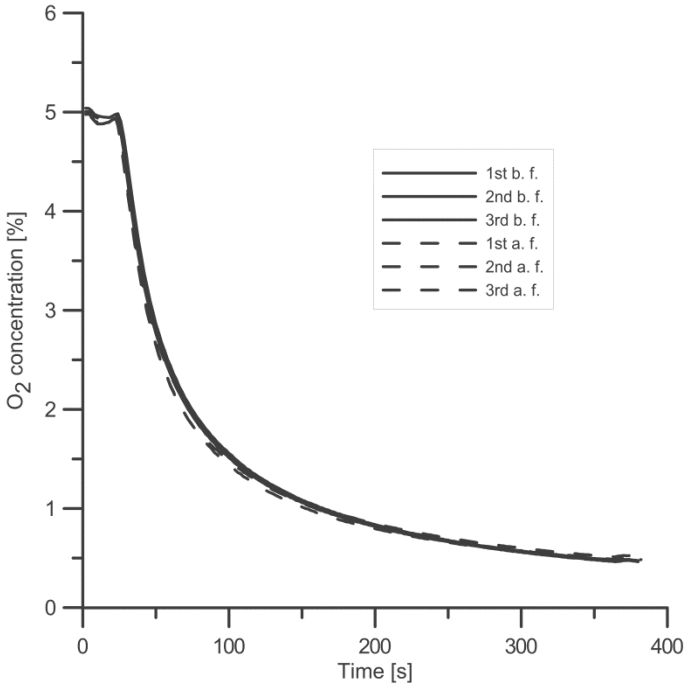

Figure 4 Oxygen release as a function of time for the nitrogen cycles at 900 °C. The solid lines represent the cycles before fuel test and the crosshatched the cycles after fuel tests. The graphs are for C10-1200 but looked similar for the other materials.

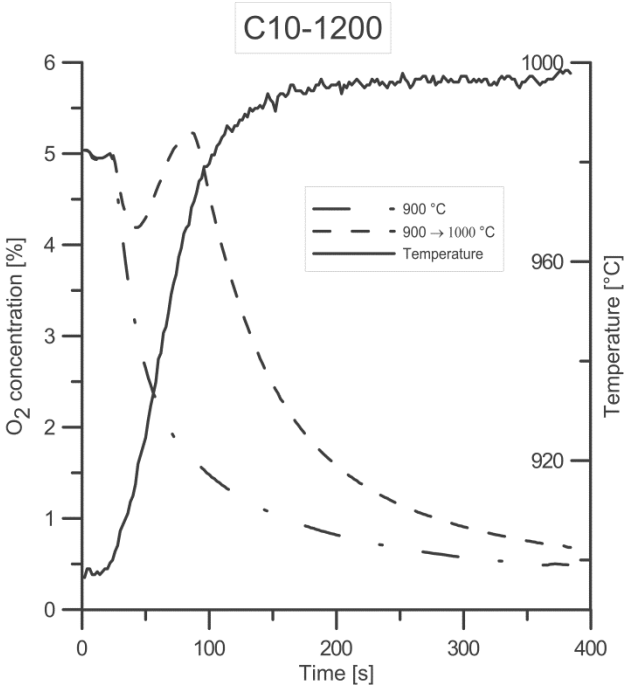

Figure 5 Oxygen release and temperature as a function of time. Comparison between a nitrogen period at 900 °C and a nitrogen period in which temperature increase from 900 to 1000 °C. The temperature curve shows how the temperature increased in the latter case.

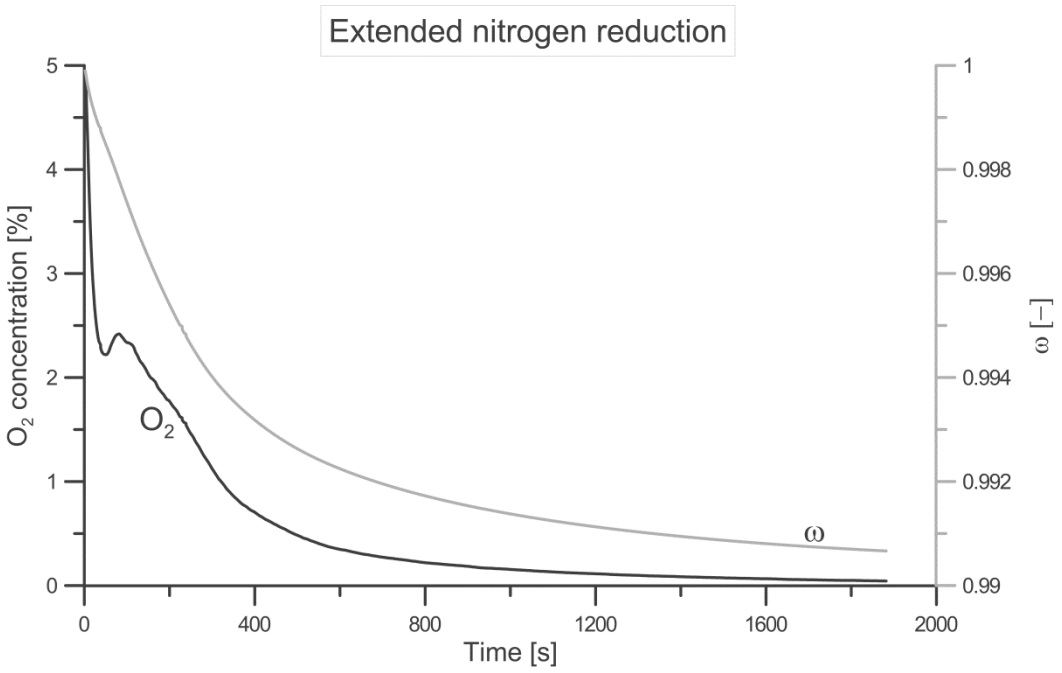

Figure 6 Oxygen release during an extended nitrogen period with temperature increased to 1000 °C. This graph is for the material C13-1300.

Reactivity with fuel

The reactivity of each material with methane at 950 °C is shown in *figure 7,* as fuel conversion (γ) as a function of degree of oxidation (ω). The particles calcined at lower temperatures have higher methane conversion. The methane conversion of the particles calcined at 1300 °C is nevertheless very high. It can be noted that the when a reducing gas such as methane is used, the ω-value can safely be reduced to circa 0.98, which corresponds to a δ change of about 0.2.

As have been explained above, experiments with a slightly smaller fuel flow, 360 mL_N/min, were also carried out with the C13 and C14 materials (*figure 8*). All particles examined managed to fully convert syngas throughout the whole syngas reduction cycles. In general the differences between the tested materials were quite small and all performed well.

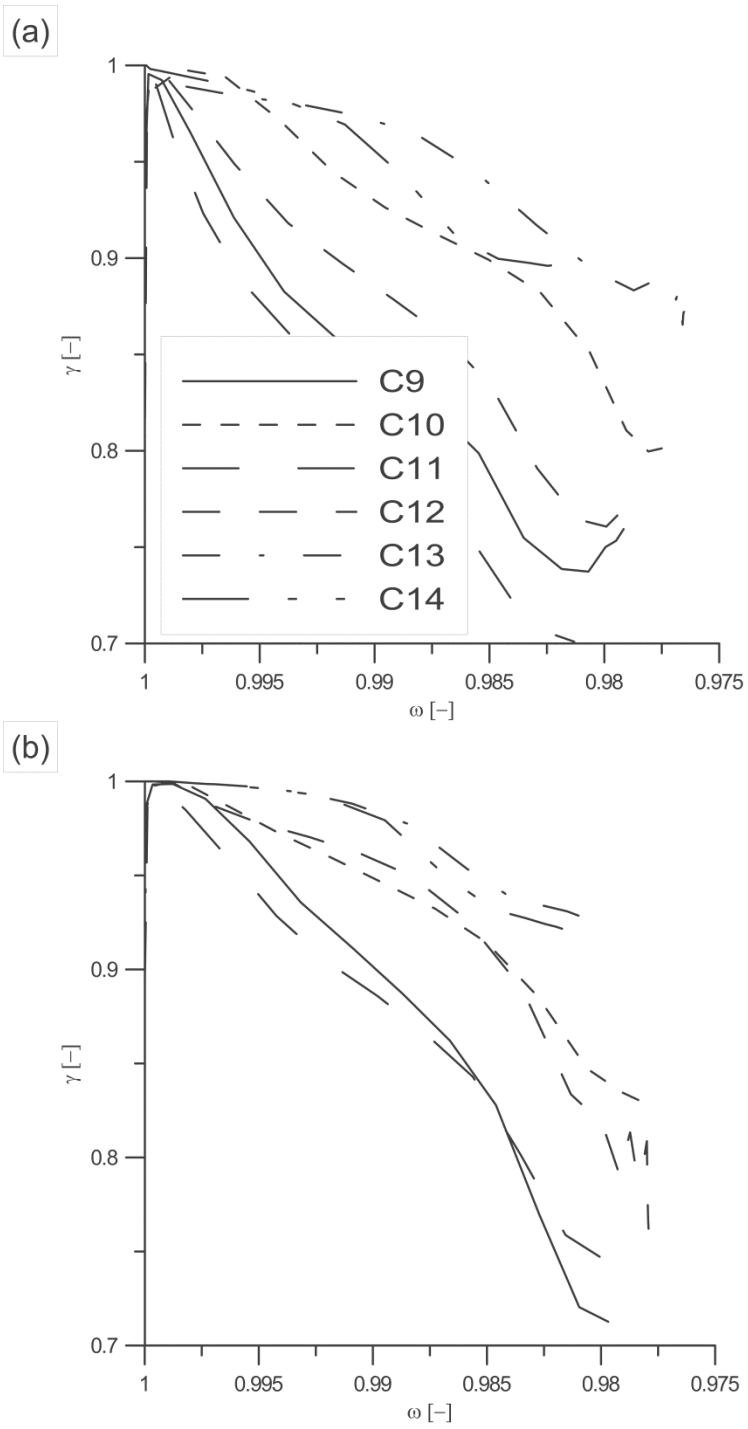
(a)
1
0.9
0.8
0.7
γ [–]
C9
C10
C11
C12
C13
C14
1
0.995
0.99
0.985
0.98
0.975
ω [–]
(b)
1
0.9
0.8
0.7
γ [–]
1
0.995
0.99
0.985
0.98
0.975
ω [–]

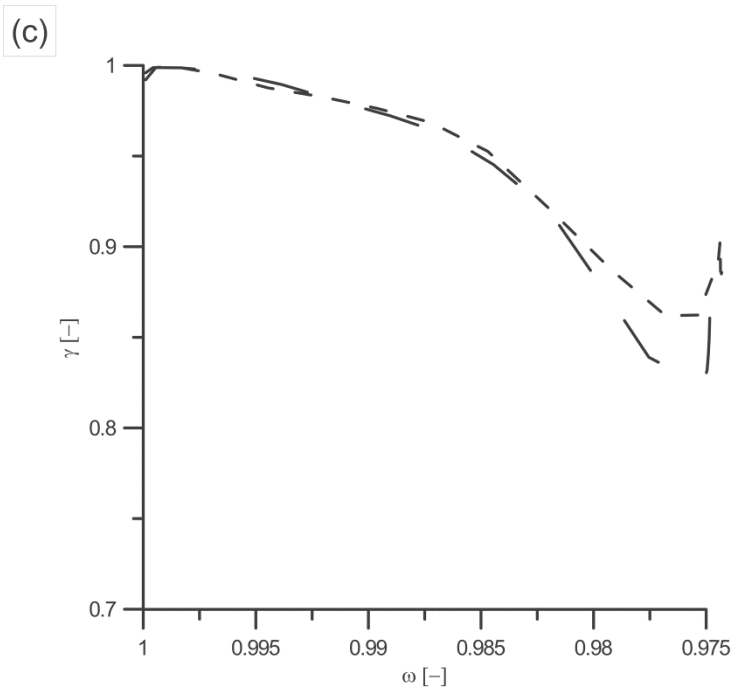

Figure 7 Reactivity with methane shown as γ against ω for particles calcined at 1300 (a), 1200 (b), 1100 °C (c). Some materials calcined at 1100°C were excluded from testing due to poor crushing strength. This is the second of the three methane reductions presented in *table 2.*

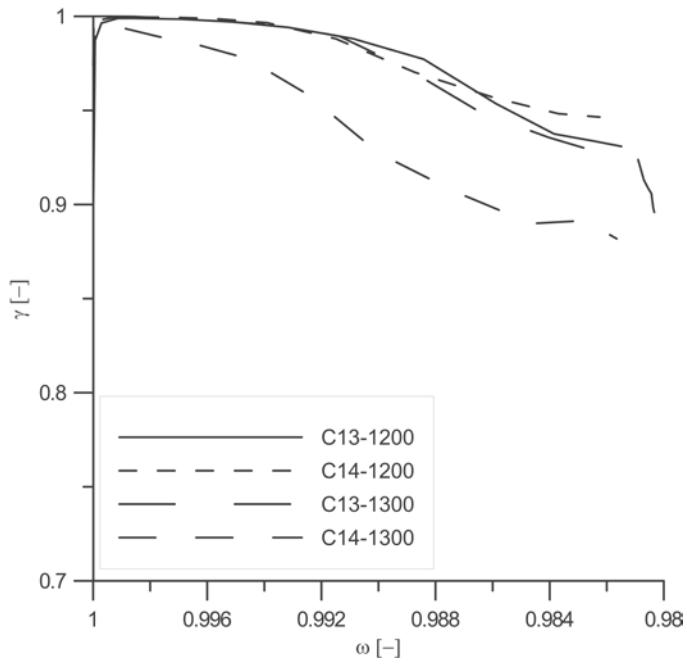

Figure 8 Reactivity with methane shown as γ as a function of ω for particles calcined at 1300 °C. In these cases a methane flow of 360 mL_N/min was used.

XRD Analysis

Both fresh oxidized particles and particles exposed to the reaction scheme outlined in table 2 were examined by X-ray diffractometry. All fresh samples consisted mainly of perovskite structures similar to $CaMnO_{3-\delta}$. Most fresh and all used samples also contained minor amounts of $CaMn_2O4$ as a separate phase. The titanium and iron oxides in C9 - C12 were found to be incorporated in the perovskite structure, in phases identified as for example $CaMn_{0.7}Ti_{0.3}O_{3-\delta}$ and $CaMn_{0.7}Fe_{0.3}O_{3-\delta}$ .The lack of free Fe_2O_3 or TiO_2 in all but one sample also verifies that iron and titanium was included in the perovskite structure. In C13 and C14 the magnesium oxide were found as a separate MgO phase. XRD results are presented in *table 4*.

Table 4 Phases identified from XRD. Fresh and used indicates whether the particles have been tested in batch reactor or not. Particles calcined at 1100 °C were of little interest due to very low crushing strength and have not been tested.

Particle	Sint. Temp.	fresh	used
C9	1200	$Ca(Mn,Ti)O_{3-\delta}$, $CaMn_2O_4$	$Ca(Mn,Ti)O_{3-\delta}$, $CaMn_2O_4$
	1300	$Ca(Mn,Ti)O_{3-\delta}$, $CaMn_2O_4$	$Ca(Mn,Ti)O_{3-\delta}$, $CaMn_2O_4$
C10	1200	$Ca(Mn,Ti)O_{3-\delta}$, $CaMn_2O_4$	$Ca(Mn,Ti)O_{3-\delta}$, $CaMn_2O_4$
	1300	$Ca(Mn,Ti)O_{3-\delta}$, $CaMn_2O_4$	$Ca(Mn,Ti)O_{3-\delta}$, $CaMn_2O_4$
C11	1200	$Ca(Mn,Fe)O_{3-\delta}$, $CaMn_2O_4$	$Ca(Mn,Fe)O_{3-\delta,}$ $CaMn_2O_4$
	1300	$Ca(Mn,Fe)O_{3-\delta}$, $CaMn_2O_4$, Fe_2O_3	$Ca(Mn,Fe)O_{3-\delta}$, $CaMn_2O_4$
C12	1200	$Ca(Mn,Fe)O_{3-\delta}$, $CaMn_2O_4$	$Ca(Mn,Fe)O_{3-\delta}$, $CaMn_2O_4$
	1300	$Ca(Mn,Fe)O_{3-\delta}$	$Ca(Mn,Fe)O_{3-\delta}$, $CaMn_2O_4$

C13	1200	MgO, $CaMnO_{3-\delta}$	MgO, $CaMnO_{3-\delta}$, $CaMn_2O_4$
	1300	MgO, $CaMnO_{3-\delta}$	MgO, $CaMnO_{3-\delta}$, $CaMn_2O_4$
C14	1200	$CaMnO_{3-\delta}$, $CaMn_2O_4$	$CaMnO_{3-\delta}$, $CaMn_2O_4$, MgO
	1300	$CaMnO_{3-\delta}$, MgO	$CaMnO_{3-\delta}$, MgO, $CaMn_2O_4$

Discussion

Most research about the CLOU process focus on the use of CuO based oxygen carrier materials. There are several reasons to examine manganese-based materials though. Manganese is almost one order of magnitude cheaper than copper and more readily available. It is also magnetic which may be useful to separate the oxygen carrier from coal ash.

Generally speaking, it should possible to release up to 3.4 wt% gas phase O_2 from pure Mn_2O_3 by reduction to Mn_3O_4. Most often this reaction has not proven to be feasible in reality due to the very slow reoxidation of Mn_3O_4 at relevant temperatures.

Adding Ca to form $CaMnO_{3-\delta}$ seems like a possible way around this dilemma. The oxygen carrier materials examined in this study have very good reactivity with CH_4 and are capable of releasing O_2 in gas phase. However, the amount of gas phase O_2 released only amounts to about 1 wt%. It is thus clear that at least half of the oxygen provided for methane oxidation comes from gas-solid reactions with the oxygen carrier rather than gas-gas reactions with gas phase oxygen. These materials are therefore best suited for gaseous fuel applications where the oxygen carrying capacity is utilized properly.

Partial substitution of perovskite materials is common practice in many applications and is well known to influence the properties of such materials. In general, addition of different dopants or could be expected to affect the O_2-conductivity of the perovskite. Also, the B site in a perovskite is often catalytically active. Previous studies have shown that addition of Ti to

CaMnO3 helps inhibit coke formation and prevent decomposition into spinel structure[15]. This study suggests that also the reactivity with fuel can be improved, at least to some extent.

Conclusions

It can be concluded that spray dried particles of perovskite structure appears to be feasible and, in fact, highly interesting as oxygen carrier for chemical looping combustion with oxygen uncoupling. Not only did such material prove to release gas phase O_2, but the reactivity during direct reduction with methane and syngas was also very high. $CaMnO_{3-\delta}$ appears to be a very promising base composition for such materials and it is clear that it is possible to incorporate small amounts of other ions in the structure as well, which may provide a possibility to optimize or improve material properties and performance. To summarize;

Six different material compositions based on the formula $CaMn_{(1-x)}M_xO_{3-\delta}$ (M=Ti, Fe, Mg) were tested, all of which showed to have a substantial CLOU effect. The particles released 0.3 – 0.5 % of total mass to inert atmosphere in 360 seconds at 900 °C.

Increased temperature facilitated the release of O_2. In 1800 s at 1000 °C oxygen corresponding to around 1 % of the total particle mass was released.

All materials showed high or full conversion of methane as well as full conversion of syngas at 950°C.

Particles doped with Mg and calcined at 1300°C provided high fuel conversion, high crushing strength and maintained good fluidization behaviour. Compared with similar particles examined by Leion et al.[15] these showed similar fuel conversion and oxygen release although oxidized at a lower oxygen concentration.

XRD analysis showed that all materials were of perovskite structure. This was true for both fresh and used samples. Fe and Ti were incorporated in the perovskite structure, while Mg existed as free MgO. Most sample also contained small amounts of $CaMn_2O_4$, which while undesired does not seem to have hampered the overall performance of the particles.

Corresponding Author

*Peter Hallberg, peter.hallberg@chalmers.se

ACKNOWLEDGMENT

The research leading to these results has received funding from the European Union Seventh Framework Programme (FP7/2007-2013) under grant agreement n° 241401. Also, Ali Hedayati is acknowledged for having performed parts of the experimental work involving particles calcined at 1100°C.

REFERENCES

1. Lyngfelt, A., B. Leckner, and T. Mattisson, A fluidized-bed combustion process with inherent CO2 separation; application of chemical-looping combustion. *Chemical Engineering Science*, **2001**. *56(10)*, 3101-3113.

2. Lyngfelt, A. Oxygen Carriers for Chemical Looping Combustion – 4000 h of Operational Experience. *Oil & Gas Science and Technology – Rev. IFP Energies nouvelles*, **2011**, *66(2)*, 161-172

3. Mattisson, T., A. Lyngfelt, and H. Leion, Chemical-looping with oxygen uncoupling for combustion of solid fuels. *International Journal of Greenhouse Gas Control*, **2009**. *3(1),* 11-19.

4. Mattisson, T., H. Leion, and A. Lyngfelt, Chemical-looping with oxygen uncoupling using CuO/ZrO_2 with petroleum coke. *Fuel*, **2009**. *88(4),* 683-690.

5. Lyngfelt, A. and T. Mattisson, Trestegsförbränning för avskiljning av koldioxid. 2005. Patent application. Sweden.

6. Mattisson, T., M. Johansson, and A. Lyngfelt. Chemial-looping with oxygen uncoupling for combustion of solid fuels. *Int. Jour. Of Greenhouse Gas Control.* **2009.** *3(1)*, 11-19.

7. Hossain, M.M. and H.I. de Lasa, Chemical-looping combustion(CLC) for inherent CO_2 separation – A review. *Chemical Engineering Science*, **2008**. *63*, 4433-4451.

8. Adanez, J., L.F. de Diego, F. Garcia-Labiano, P. Gayan, A. Abad, and J.M. Palacios, Selection of Oxygen Carriers for Chemical-Looping Combustion. *Energy & Fuels*, **2004**. *18(2),* 371-377.

9. Jerndal, E., T. Mattisson, and A. Lyngfelt, Investigation of Different NiO/NiAl(2)O(4) Particles as Oxygen Carriers for Chemical-Looping Combustion. *Energy & Fuels*, **2009**. *23(1),* 665-676.

10. Linderholm, C., A. Abad, T. Mattisson, and A. Lyngfelt, 160 h of chemical-looping combustion in a 10 kW reactor system with a NiO-based oxygen carrier. *International Journal of Greenhouse Gas Control*, **2008**. *2(4),* 520-530.

11. Linderholm, C., A. Shulman, T. Mattisson, and A. Lyngfelt, High Reactivity and Mechanical Durability of NiO/NiAl(2)O(4) and NiO/NiAl(2)O(4)/MgAl(2)O(4) Oxygen Carrier

Particles Used for more than 1000 h in a 10 kW CLC Reactor. *Industrial & Engineering Chemistry Research*, **2009**. *48(15),* 7400-7405.

12. Bolhàr-Nordenkampf, J., T. Pröll, P. Kolbitsch, and H. Hofbauer, Performance of a NiO-based oxygencarrier for chemical looping combustion and reforming in a 120 kW unit. *Energy Procedia*, **2009**. *1(1),* 19 – 25.

13. Adánez, J., Dueso, C., Diego, L.F.D., García-Labiano, F., Gayán, P., Abad, A., Methane combustion in a 500 Wth chemical-looping combustion system using an impregnated ni-based oxygen carrier. *Energy and Fuels*, **2009**. *23(1),* 130-142.

14. Adanez J., Abad A., Garcia-Labiano F., Gayan P., de Diego L.F., Progress in Chemical-Looping Combustion and Reforming technologies, *Progress in Energy and Combustion Science*. **2012.** *38*, 215-282

15. Leion, H., Y. Larring, E. Bakken, R. Bredesen, T. Mattisson, and A. Lyngfelt, The use of $CaMn_{0.875}Ti_{0.125}O_3$ as oxygen carrier in Chemical-Looping with Oxygen Uncoupling (CLOU). *Energy & Fuels*, **2009**. *23,* 5276-5283.

16. Rydén, M., A. Lyngfelt, and T. Mattisson, $CaMn_{0.875}Ti_{0.125}O_3$ as oxygen carrier for chemical-looping combustion with oxygen uncoupling (CLOU) – experiments in continuously operating fluidized bed reactor system. *International Journal of Greenhouse gas control.* **2011,** *5(2),* 356-366.

17. Fossdal, A., E. Bakken, B.A. Øye, C. Schøning, I. Kaus, T. Mokkelbost, and Y. Larring, Study of inexpensive oxygen carriers for chemical looping combustion. *International Journal of Greenhouse Gas Control*, **2011**. *5(3),* 483-488.

18. Leonidova E.I., Leonidov I.A., Patrakeev M.V., Kozhevnikov V.L., Oxygen non-stoichiometry, high-temperature properties, and phase diagram of CaMnO3–δ, *Journal of Solid State Electrochemistry*. **2011.** *15*, 1071-1075

19. Li C., Soh K.C.K, Wu P., Formability of ABO3 perovskites, *Journal of alloys and compounds*. **2004**. *372*, 40-48

20. Rørmark L., Mørch A.B., Wiik K., Stølen S., Grande T., Enthalpies of oxidation of CaMnO3-δ, Ca2MnO4-δ and SrMnO3-δ – deduced redox properties, *Chemistry of Materials*. **2001**. *13*, 4005-4013

21. Rydén, M., Leion, H., Lyngfelt, A. & Mattisson, T. 2012, "Combined oxides as oxygen carrier material for chemical-looping combustion with oxygen uncoupling", 2nd International Conference on Chemical Looping, Darmstadt, Germany, September 2012

22. Sarshar, Z., Sun, Z., Zhao, D., Kaliaguine, S. Development of sinter-resistant core-shell LaMn xFe 1- xO 3@mSiO 2 oxygen carriers for chemical looping combustion *Energy and Fuels*. **2012**. *26 (5)* 3091-3102

23. Nalbandian, L., Evdou, A., Zaspalis, V. La1-xSrxMyFe1-yO 3-δ perovskites as oxygen-carrier materials for chemical-looping reforming. *International Journal of Hydrogen Energy* **2011**. *36 (11)*. 6657-6670

24. Bakken, E., Norby, T., Stoelen, S. Nonstoichiometry and reductive decomposition of $CaMnO_{3-\delta}$. *Solid State Ionics*, **2004**, *176 (1-2)*, 217–223

25. Azimi, G., H. Leion, T. Mattisson, and A. Lyngfelt. Chemical-looping with oxygen uncoupling for Mn-based materials, testing in batch fluidized bed. *Energy Procedia,* **2011,** *4,* 370-377